SUPPLEMENTARY INFORMATION

Supplementary Figure 1-13

Supplementary Table 1: Genotypes by figures

Supplementary Table 2: Primers used in this study

SUPPLEMENTARY FIGURES

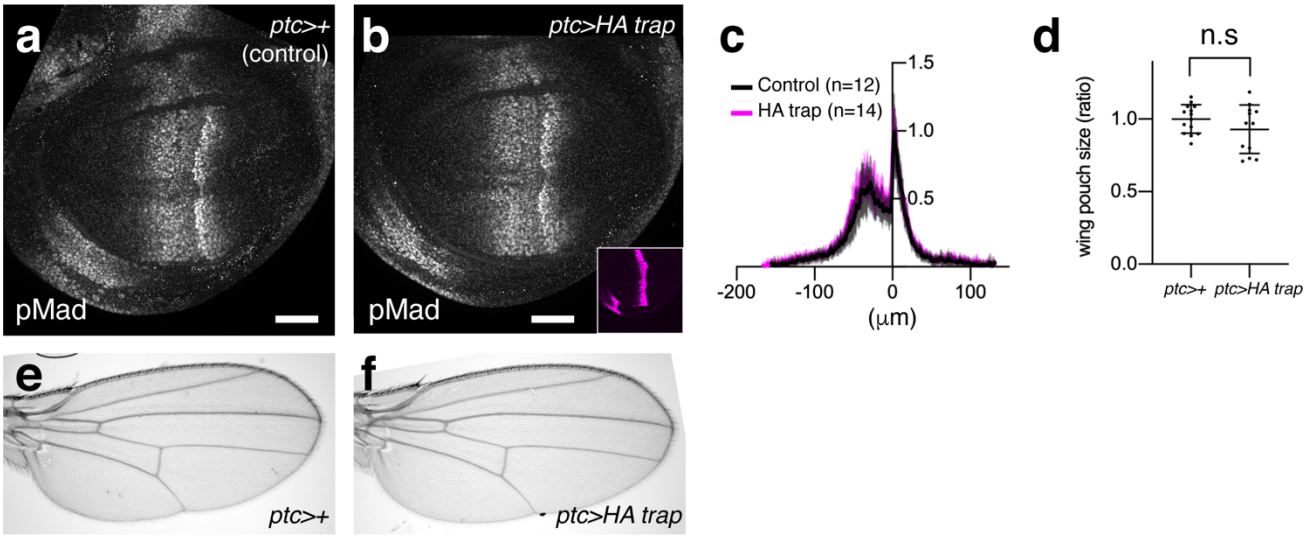

Supplementary Fig 1. Expression of HA trap using *ptc*-Gal4 did not affect Dpp signaling or patterning and growth of the adult wing in the absence of a HA-tagged protein.
a-b, pMad staining of *ptc*>+ wing disc (control) (**a**), and *ptc*>*HA trap* wing disc (**b**). Scale bar 50 μm. **c**, Average fluorescence intensity profile of α-pMad staining of (**a**-**b**). *ptc*>+ wing disc (control) (*n*=12), and *ptc*>*HA trap* wing disc (*n*=14). Data are presented as mean+/-SD. **d**, Comparison of wing pouch size of (**a**-**b**). *ptc*>+ wing disc (control) (*n*=14) and *ptc*>*HA trap* wing disc (*n*=12). Data are presented as mean+/-SD. Two-sided unpaired Student's *t*-test with unequal variance was used (*p*=0.211). (n.s; not significant). **e-f**, Adult wing of *ptc*>+ (**e**), and *ptc*>*HA trap* (**f**).

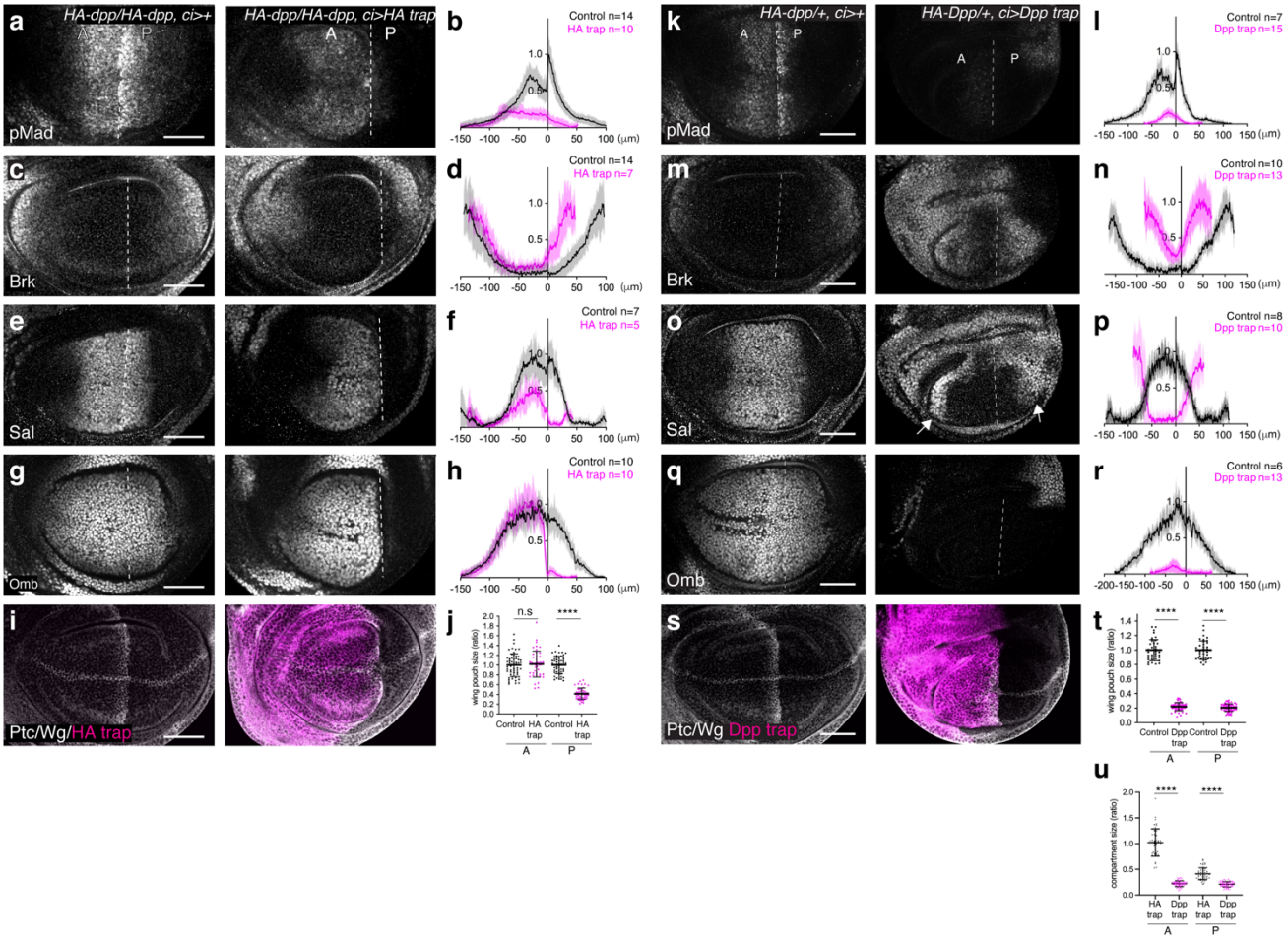

Supplementary Fig 2. Patterning and growth defects by HA trap and Dpp trap expression using *ci-Gal4*

a–**j**, Patterning and growth defects by HA trap. (**a**, **c**, **e**, **g**, **i**) α-pMad (**a**), α-Brk (**c**), α-Sal (**e**), α-Omb (**g**), α-Ptc/Wg staining and HA trap (mCherry) (**i**) of control *HA-dpp/HA-dpp, ci>+* (left) and *HA-dpp/HA-dpp, ci>HA* trap (right). (**b**, **d**, **f**, **h**) Average fluorescence intensity profile of (**a**, **c**, **e**, **g**) respectively. Data are presented as mean+/-SD. (**j**) Comparison of compartment size of *HA-dpp/HA-dpp, ci>+* wing pouch (control) (*n*=56) and *HA-dpp/HA-dpp, ci>HA* trap wing pouch (*n*=47). Data are presented as mean+/-SD. Two-sided Mann-Whitney test was used for comparison of the A compartment size (p=0.8355). (n.s; not significant) Two-sided unpaired Student's *t*-test with unequal variance was used for comparison of the P compartment size (p<0.0001). (****p<0.0001). **k**-**t**, Patterning and growth defects by Dpp trap. (**k**, **m**, **o**, **q**, **s**) α-pMad (**k**), α-Brk (**m**), α-Sal (**o**), α-Omb (**q**), α-Ptc/Wg staining and HA trap (mCherry) (**s**) of control *HA-dpp/+, ci>+* (left) and *HA-dpp/+, ci>Dpp* trap (right). (**l**, **n**, **p**, **r**) Average fluorescence intensity profile of (**k**, **m**, **o**, **q**) respectively. Data are presented as mean+/-SD. **t**, Comparison of each compartment size of *HA-dpp/+, ci>+* wing pouch (control) (*n*=37) and *HA-dpp/+, ci>Dpp* trap wing pouch (*n*=53). Data are presented as mean+/-SD. Two-sided unpaired Student's *t*-test with unequal variance was used for comparison of the A compartment size (p<0.0001) and for comparison of the P compartment size (p<0.0001). (****p<0.0001). **u**, Comparison of normalized compartment size of wing pouch upon HA trap (*n*=47) and Dpp trap (*n*=53) expression using *ci-Gal4* (the same data set from Supplementary Fig. 2j and Supplementary Fig. 2t). Data are presented as mean+/-SD. Two-sided Mann-Whitney test was used for comparison of the A compartment size (p<0.0001). Two-sided unpaired Student's *t*-test with unequal variance was used for comparison of the P compartment size (p<0.0001). Dashed white lines mark the A-P compartment border. Scale bar 50 μm.

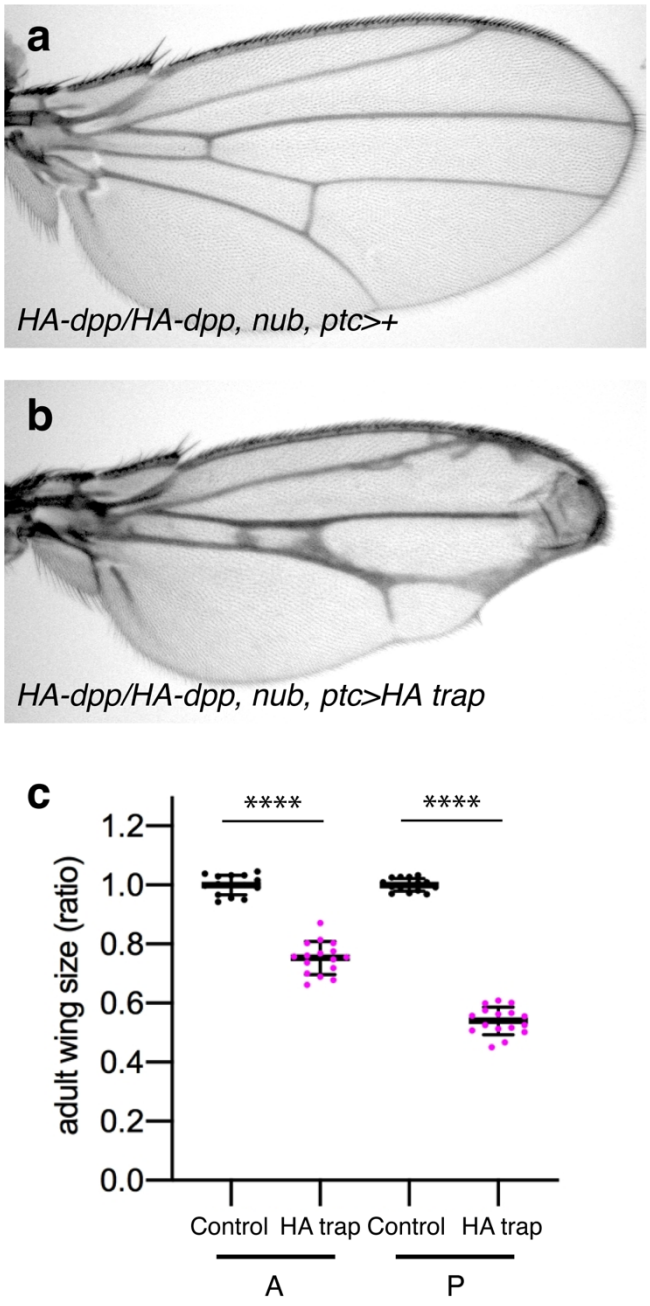

Supplementary Fig 3. Patterning and growth defects by concomitant HA trap expression using *ptc-Gal4* and *nub-Gal4*

a-**b**, Adult wing of control *HA-dpp/HA-dpp, nub, ptc>+* (**a**), and *HA-dpp/HA-dpp, nub, ptc>HA trap* (**b**). **c**, Comparison of compartment size of (**a**-**b**). *HA-dpp/HA-dpp, nub, ptc>+* adult wing (*n*=15) and *HA-dpp/HA-dpp, nub, ptc>HA trap* adult wing (*n*=16). Data are presented as mean+/-SD. Two-sided unpaired Student's *t*-test with unequal variance was used for comparison of the A compartment size ($p<0.0001$) and for comparison of the P compartment size ($p<0.0001$). (****$p<0.0001$). Note that patterning and growth defects were not enhanced by concomitant HA trap expression using *ptc-Gal4* and *nub-Gal4*.

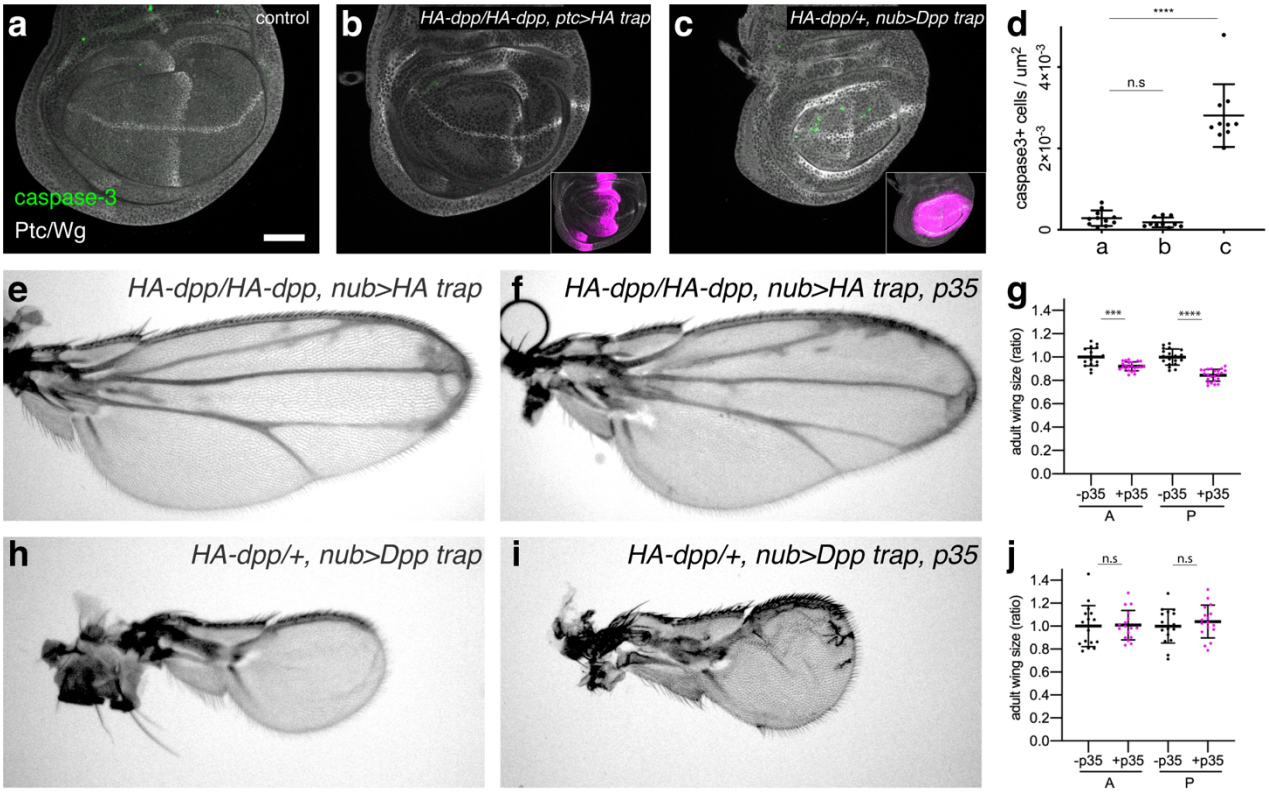

Supplementary Fig 4. Blocking cell death does not rescue growth defects caused by HA trap or Dpp trap

a-d, α-Caspase-3 and α-Ptc/Wg staining of control wing disc (**a**), *HA-dpp/HA-dpp, ptc>HA trap* wing disc (**b**), and *HA-dpp/+, nub>Dpp trap* wing disc (**c**). The insets show HA trap or Dpp trap (mCherry) expression. Scale bar 50 μm. Note that wing discs where HA trap was expressed using *ptc*-Gal4 and wing discs where Dpp trap was expressed using *nub*-Gal4 were analyzed since each condition showed the most severe phenotypes among Gal4 lines used. (**d**) Comparison of the number of α-Caspase-3 positive cells of (**a-c**). Control wing disc (**a**, n=11), *HA-dpp/HA-dpp, ptc>HA trap* wing disc (**b**, n=10), and *HA-dpp/+, nub>Dpp trap* wing disc (**c**, n=10). Data are presented as mean+/-SD. Two-sided unpaired Student's t-test with unequal variance was used for comparison between (**a**) and (**b**) (p=0.1541). (n.s; not significant). Two-sided Mann-Whitney test was used for comparison between (**a**) and (**c**) (p<0.0001). (****p<0.0001). **e-f**, Adult wing of *HA-dpp/HA-dpp, nub>HA trap* (control) (**e**) and *HA-dpp/HA-dpp, nub>HA trap, p35* (**f**). **g**, Comparison of compartment size of (**e-f**). *HA-dpp/HA-dpp, nub>HA trap* adult wing (n=19) and *HA-dpp/HA-dpp, nub>HA trap, p35* adult wing (n=23). Data are presented as mean+/-SD. Two-sided unpaired Student's t-test with unequal variance was used for comparison of the A compartment size (p=0.0003) and for comparison of the P compartment size (p<0.0001). (***p<0.001, ****p<0.0001). **h-i**, Adult wing of *HA-Dpp/+, nub>Dpp trap* (control) (**h**) and *HA-dpp/+, nub>Dpp trap, p35* (**i**). **j**, Comparison of compartment size of (**h-i**). *HA-Dpp/+, nub>Dpp trap* adult wing (n=17) and *HA-dpp/+, nub>Dpp trap, p35* adult wing (n=17). Data are presented as mean+/-SD. Two-sided unpaired Student's t-test with unequal variance was used for comparison of the A compartment size (p=0.8750) and for comparison of the P compartment size (p=0.4260). (n.s; not significant).

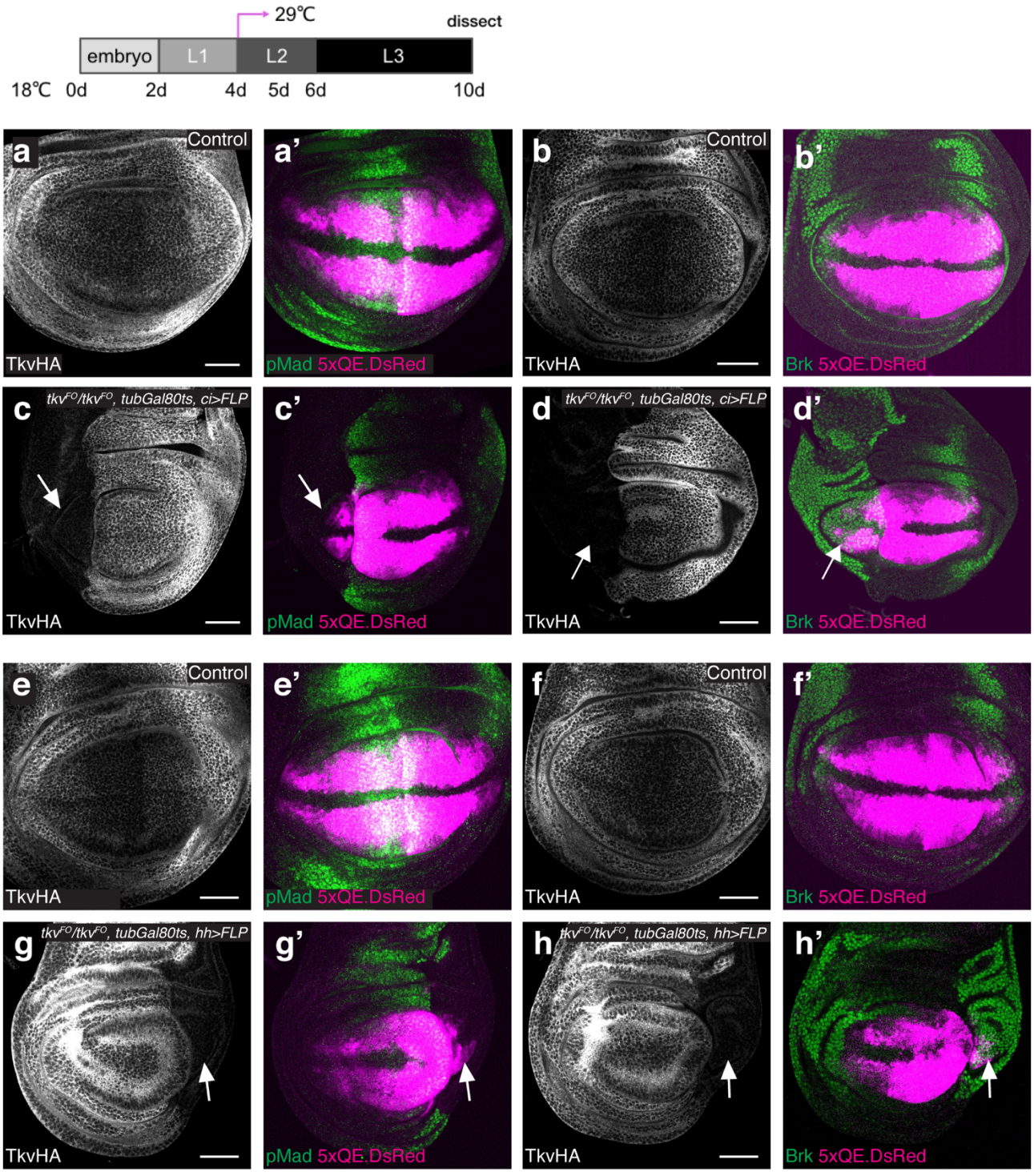

Supplementary Fig 5. *5xQE.DsRed* remains expressed in each compartment where *tkv* is genetically removed from the beginning of second instar stage.

a-d, α-HA (TkvHA^{FO}) staining (**a-d**) and α-Brk staining and 5xQE.DsRed expression (**a'-d'**) of control wing disc (**a**, **b**) and *5xQE.DsRed, tkvHA^{FO}/tkvHA^{FO}, tubGal80ts, ci>UAS-FLP* (**c**, **d**). **e-h**, α-HA (TkvHA^{FO}) staining (**e-h**) and α-Brk staining and 5xQE.DsRed expression (**e'-h'**) of control wing disc (**e**, **f**) and *5xQE.DsRed, tkvHA^{FO}/tkvHA^{FO}, tubGal80ts, hh>UAS-FLP* (**g**, **h**). Crosses were shifted from 18°C to 29°C at 4 day AEL (early second instar). Arrows indicate 5xQE.DsRed expression in the compartment where *tkv* is genetically removed. Scale bar 50 μm.

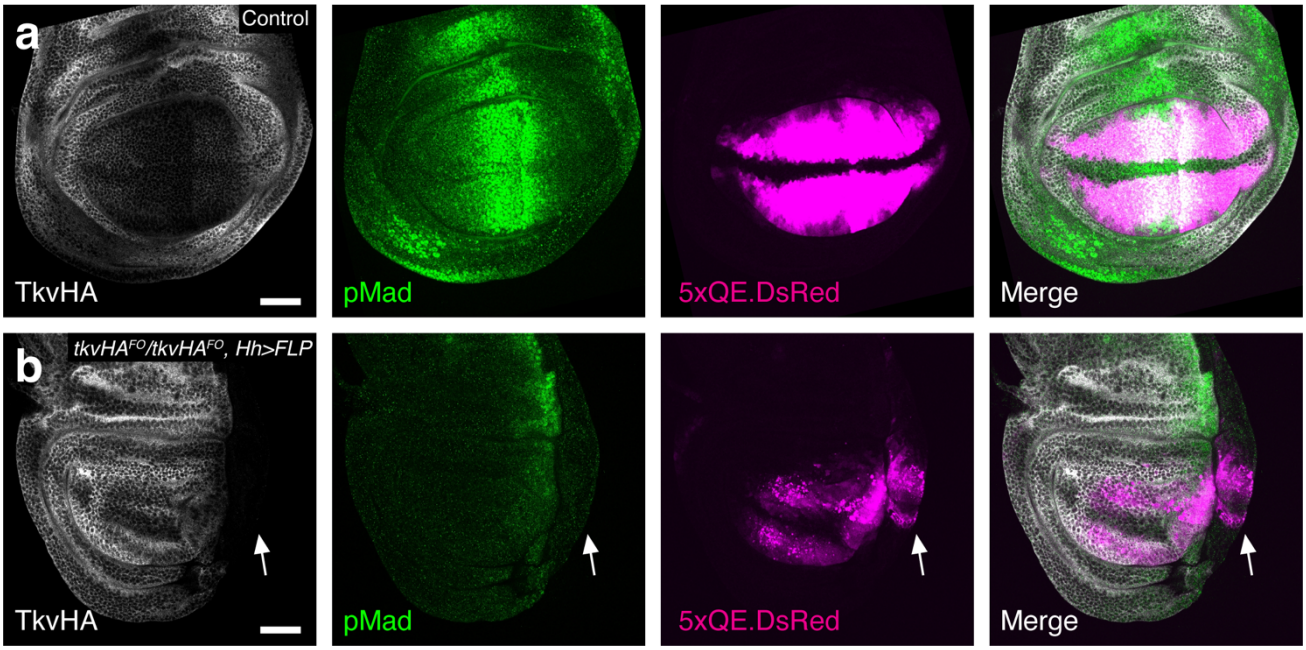

Supplementary Fig 6. A part of posterior wing pouch can grow without *tkv*.
a-**b**, α-HA (TkvHA^{FO}), α-pMad, 5xQE.DsRed, and merge of control wing disc (**a**), and wing disc where *tkv* is genetically removed from the entire P compartment using *Hh*-Gal4 (**b**). Upon removal of *tkv* from the P compartment, the 5xQE.DsRed reporter remained expressed in the P compartment (arrow) despite complete loss of pMad signal and severe growth defects in the P compartment. Note that anterior pMad signal was also affected probably because Hh target *dpp* expression is affected by the reduced number of Hh producing posterior cells. Scale bar 50 μm.

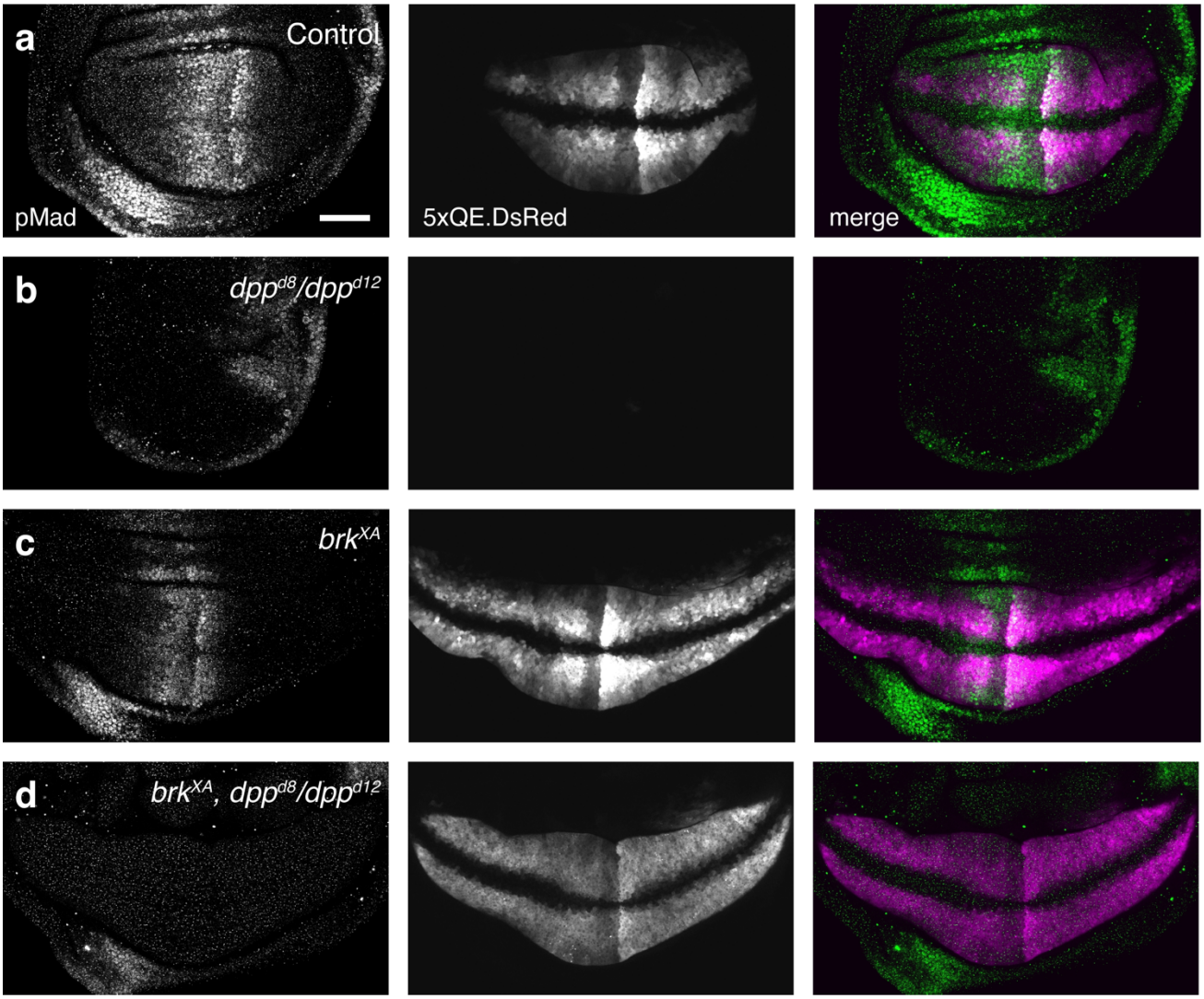

Supplementary Fig 7. *5xQE.DsRed* reporter expression is largely independent of Dpp signaling
a-d, α-pMad, 5xQE.DsRed, and merge of control (**a**), dpp^{d8}/dpp^{d12} (**b**), brk^{XA} (**c**), and brk^{XA}; dpp^{d8}/dpp^{d12} (**d**) wing discs. Scale bar 50 μm.

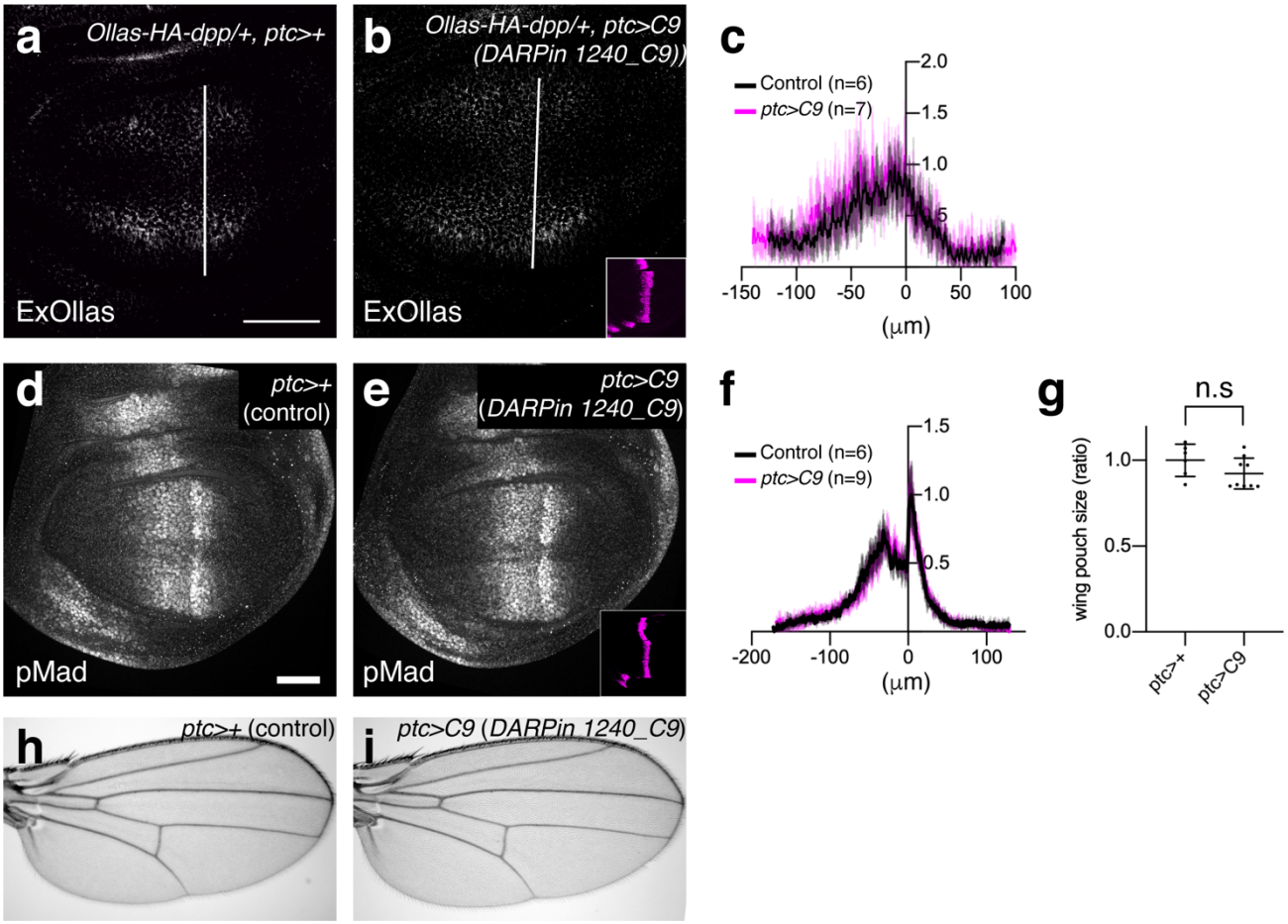

Supplementary Fig 8. Expression of a trap (containing DARPin 1240_C9) using *ptc*-Gal4 did not affect extracellular distribution of Dpp, pMad signaling, or patterning and growth of the adult wing

a-b, Extracellular α-Ollas staining (ExOllas) of *Ollas-HA-dpp/+, ptc>+* wing disc (control) (**a**), and *Ollas-HA-dpp/+, ptc>C9* wing disc (**b**). **c**, Average fluorescence intensity profile of extracellular α-Ollas staining of (**a-b**). *Ollas-HA-dpp/+, ptc>+* wing disc (control) (*n*=6), and *Ollas-HA-dpp/+, ptc>C9* wing disc (*n*=7). Data are presented as mean+/-SD. **d-e**, α-pMad of *ptc>+* wing disc (control) (**d**), and *ptc>C9* wing disc (**e**). **f**, Average fluorescence intensity profile of α-pMad staining of (**d-e**). *ptc>+* wing disc (control) (*n*=6), and *ptc>C9* wing disc (*n*=9). Data are presented as mean+/-SD. **g**, Comparison of wing pouch size of (**d-e**). *ptc>+* (control) (*n*=6), and *ptc>C9* disc (*n*=9). Data are presented as mean+/-SD. Two-sided Mann-Whitney test was used for comparison (*p*=0.0879). (n.s; not significant). **h-i**, Adult wing of *ptc>+* wing disc (control) (**h**), and *ptc>C9* (**i**). Scale bar 50 μm.

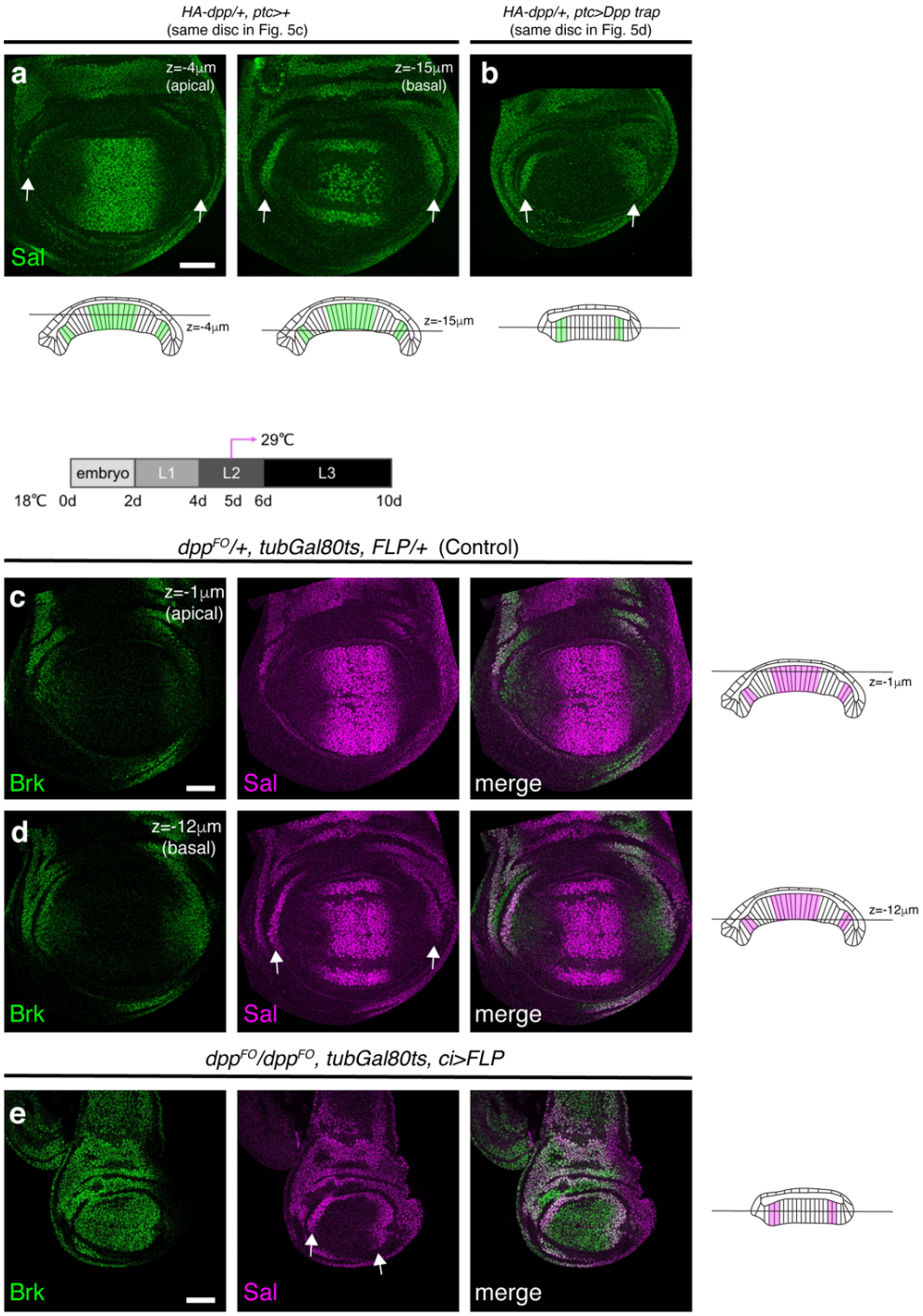

Supplementary Fig 9. Lateral Sal expression is not affected by loss of Dpp signaling
a-b, α-Sal staining of *HA-dpp/+, ptc>+* disc (control) (**a**), and *HA-dpp/+, ptc>Dpp trap* disc (**b**). Each wing disc is from Fig. 5c and Fig. 5d, respectively. In an apical confocal section of control wing disc (z=-4μm), the lateral Sal expression is hidden due to the tissue architecture but in a basal confocal section of control wing disc (z=-15μm), the lateral Sal expression is easily detected (**a**). **c-e**, α-Brk, α-Sal, and merge of dpp^{FO}/+, *tubGal80ts, FLP/+* disc (control) (**c-d,** same wing disc), and dpp^{FO}/ dpp^{FO}, *tubGal80ts, ci>FLP* disc (**e**). *dpp* was genetically removed from the mid-second instar. The lateral Sal expression is found in a basal confocal section of control wing disc (z=-12μm) (**c-d**). The lateral Sal expression is not significantly upregulated, although Brk is uniformly upregulated upon generic removal of *dpp* from the entire A compartment using *ci*-Gal4 (**e**). Scale bar 50 μm.

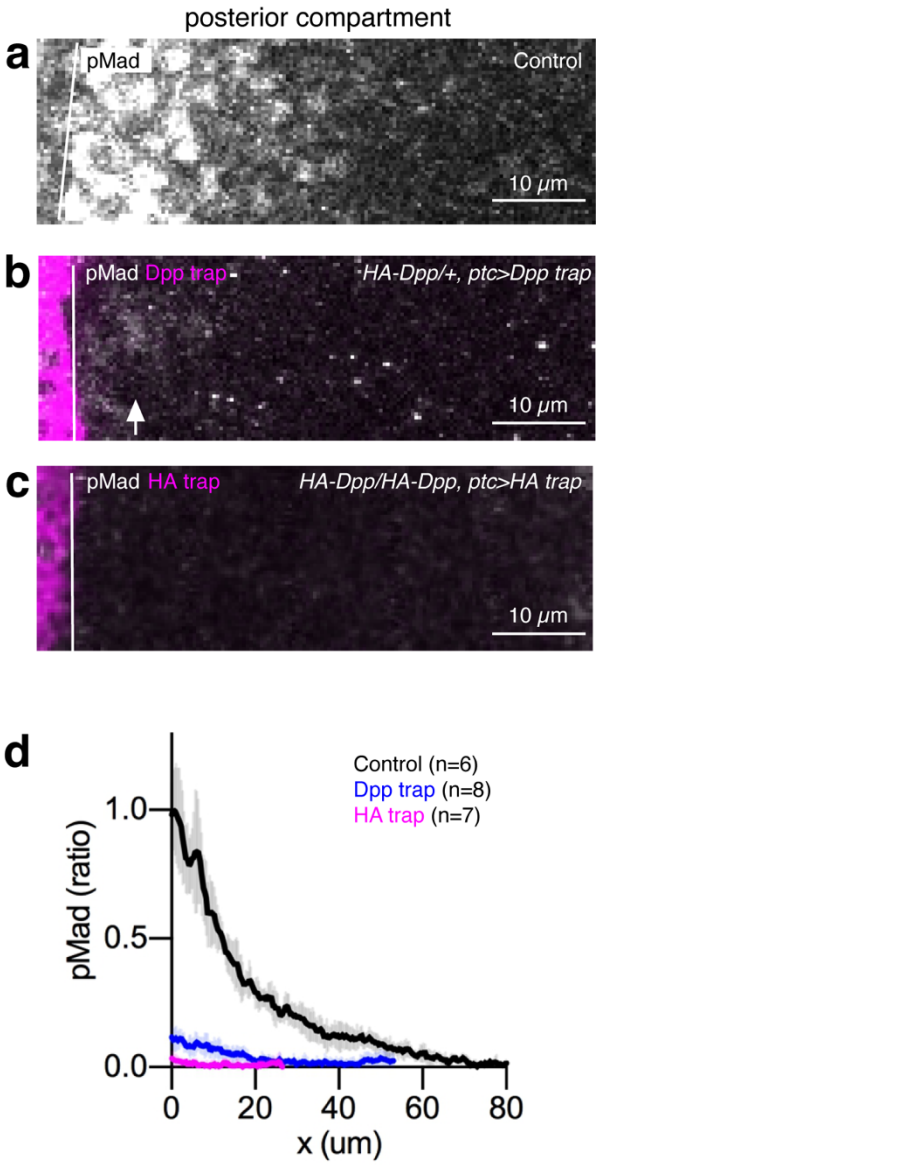

Supplementary Fig. 10. HA trap can trap Dpp more efficiently than Dpp trap
a-**c**, α-pMad and mCherry (Dpp trap or HA trap) in the P compartment of control wing disc (**a**), *HA-dpp/+, ptc>Dpp trap* wing disc (**b**), and *HA-dpp/HA-dpp, ptc>HA trap* (**c**). Scale bar 10 μm. **d**, Average fluorescence intensity profile of posterior α-pMad staining of (**a**-**c**). Data are presented as mean+/-SD. Arrow indicates pMad signal by leaked Dpp from Dpp trap.

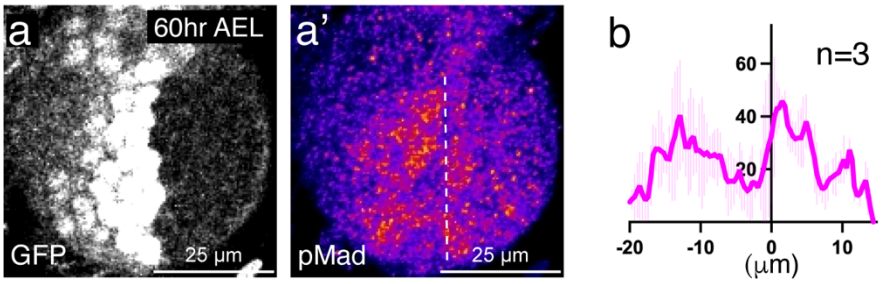

Supplementary Fig. 11. pMad signaling at mid-second instar stage
a-a', α-GFP (**a**) and α-pMad (**a'**) staining of wing disc expressing the *d2GFP* reporter at mid-second instar stage (60hr AEL). Dotted line indicates A-P compartment boundary. Scale bar 25 µm. **b**, Average fluorescence intensity profile of α-pMad staining of at mid-second instar stage (60hr AEL) (*n*=3). Data are presented as mean+/-SD.

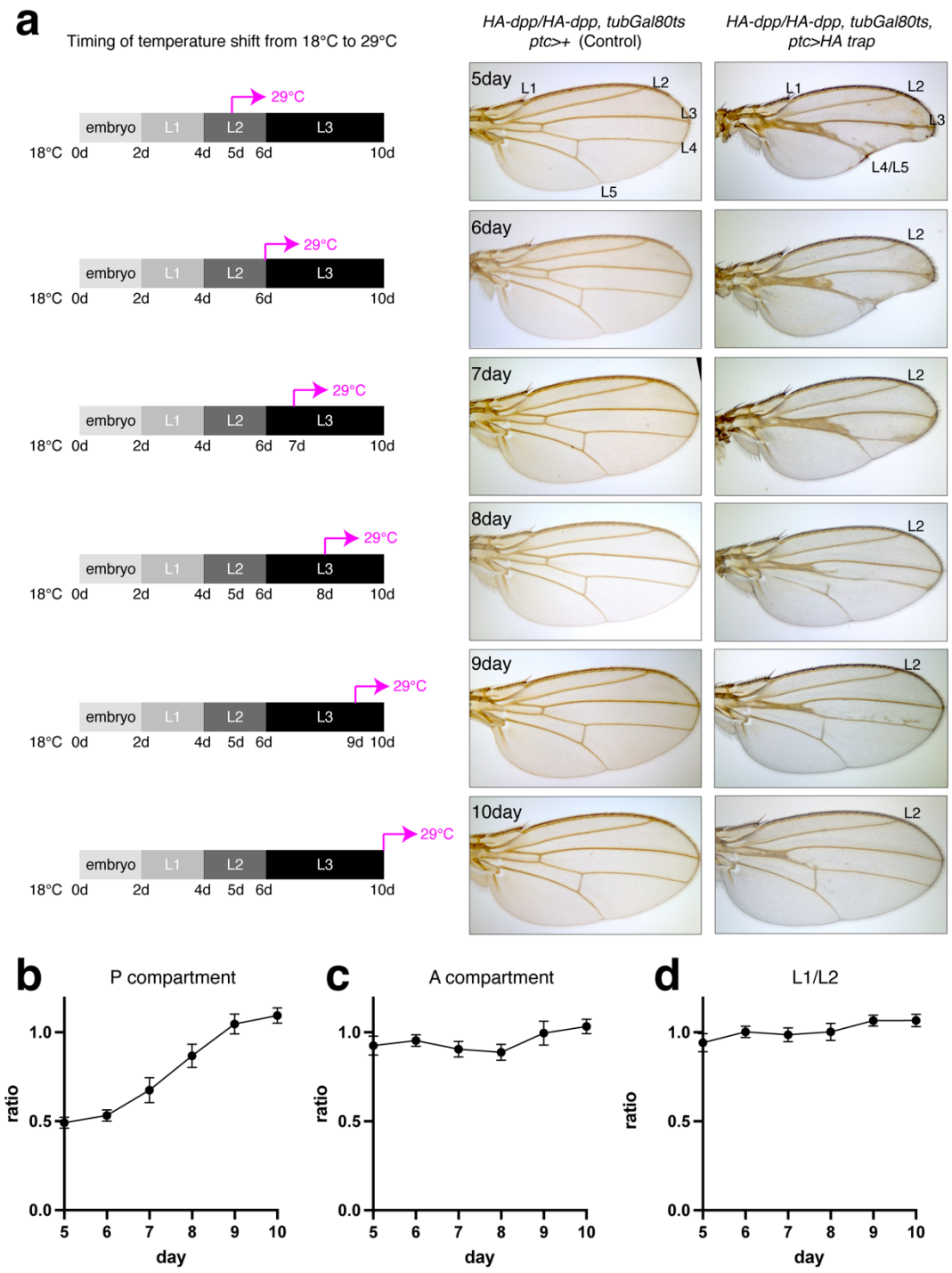

Supplementary Fig. 12 Relatively normal anterior patterning and growth by blocking Dpp dispersal at different time points

a, *HA-dpp/HA-dpp, tubGal80ts, ptc>+* control adult wings and *HA-dpp/HA-dpp, tubGal80ts, ptc>HA trap* adult wings. Crosses were shifted from 18 ℃ to 29 ℃ at indicated time point. **b**-**d**, P compartment size (**b**), A compartment size (**c**), and the size of the peripheral region between L1 and L2 (**d**) of *HA-dpp/HA-dpp, tubGal80ts, ptc>HA trap* adult wings (*n*=16, 13, 14, 24, 16, 13 at 5, 6, 7, 8, 9, 10 day) were normalized against each counter part size of *HA-dpp/HA-dpp, tubGal80ts, ptc>+* control adult wings (*n*=12, 11, 14, 13, 14, 12 at 5, 6, 7, 8, 9, 10 day). Crosses were shifted from 18 ℃ to 29 ℃ at indicated time point. Data are presented as mean+/-SD.

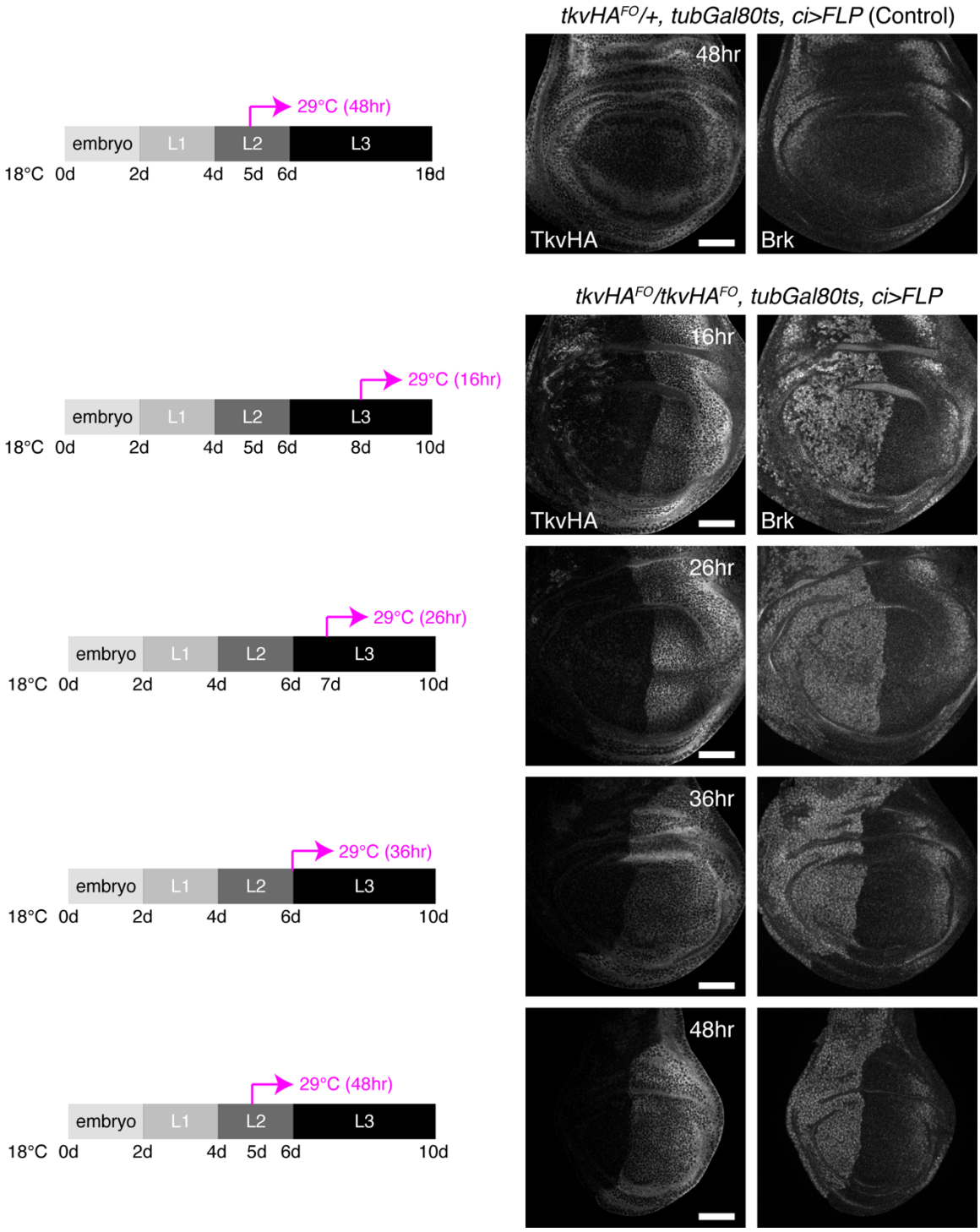

Supplementary Fig 13. De-repression of Brk by genetic removal of *tkv*

α-HA (TkvHA^{FO}) and α-Brk staining of wing discs in which *tkv* was genetically removed from A compartment using *ci*-Gal4 from different time points. The larvae were raised at 18 ℃ until a temperature shift to 29 ℃ to induce Gal4 expression. Time shown in each figure indicates the time of dissection after temperature shift. All the discs are the same age and only difference is how long *tkv* had been removed. Scale bar 50 μm.

SUPPLEMENTARY TABLE 1

Genotypes by figures

Fig. 1c-e: *yw; HA-dpp/HA-dpp*
Fig. 2b: *yw; ptc-Gal4, Ollas-HA-dpp/+*
Fig. 2d: *yw; ptc-Gal4, Ollas-HA-dpp/+; UAS/LexAop-HA trap/+*
Fig. 2f, h: *hsFLP; Ollas-HA-dpp/tub>CD2, Stop>Gal4, UAS-nlacZ; UAS/LexAop-HA trap/+*
Fig. 2j: *hsFLP; ptc-Gal4, Ollas-HA-dpp/tub>CD2, Stop>Gal4, UAS-nlacZ; UAS/LexAop-HA trap/+*
Fig. 2l: *hsFLP; Ollas-HA-dpp/tub>CD2, Stop>Gal4, UAS-nlacZ; UAS/LexAop-HA trap/+*
Fig. 3a, h: (*5xQE.DsRed); ptc-Gal4, HA-dpp/HA-dpp*
Fig. 3b, i: (*5xQE.DsRed); ptc-Gal4, HA-dpp/HA-dpp; UAS/LexAop-HA trap/+*
Fig. 3k, r: *yw; nub-Gal4, HA-dpp/HA-dpp*
Fig. 3l, s: *yw; nub-Gal4, HA-dpp/HA-dpp; UAS/LexAop-HA trap/+*
Fig. 4a: *hsFLP/5xQE.DsRed; HA-dpp, tkv^{a12} FRT40/HA-dpp, UbiGFP, FRT40, ptc-Gal4; UAS/LexAop-HA trap/+*
Fig. 4b: *hsFLP/5xQE.DsRed; tkv^{a12} FRT40/UbiGFP, FRT40*
Fig. 4c, d: *hsFLP/5xQE.DsRed; $tkvHA^{FO}$/$tkvHA^{FO}$*
Fig. 4e, f: (internal control within a cross) *5xQE.DsRed/+; (dpp^{FO}, ci-Gal4)/(dpp^{FO}); (UAS-FLP)/tubGal80ts,*
Fig. 4g, h: *5xQE.DsRed/+; dpp^{FO}, ci-Gal4/dpp^{FO}; UAS-FLP/tubGal80ts*
Fig. 5b: (left) *yw; ptc-Gal4, Ollas-HA-dpp/+*, (right) *yw; ptc-Gal4, Ollas-HA-dpp/+; UAS/LexAop-Dpp trap/+*
Fig. 5c: *yw; ptc-Gal4, HA-dpp/+*
Fig. 5d: *yw; ptc-Gal4, HA-dpp/+; UAS/LexAop-Dpp trap/+*
Fig. 5k, r: *yw; nub-Gal4, HA-dpp/+*
Fig. 5l, s: *yw; nub-Gal4, HA-dpp/+; UAS/LexAop-Dpp trap/+*
Fig. 6a, c: (*y)w; (5xQE.DsRed); dpp^{d8}/dpp^{d12}*
Fig. 6b, d: (*y)w; (5xQE.DsRed); dpp^{d8}/dpp^{d12}; dpp-Gal4/UAS-tkvQD*
Fig. 6f: (*5xQE.DsRed); dpp^{d8}, UAS-FLP/dpp^{d12}, act>Stop, y+>$LexA^{LHG}$; dpp-Gal4/LexAop-tkvQD*
Fig. 7c: *yw; dpp-T2A-Gal4, Dp(2;2)DTD48(dpp+)/+; P{w[+mC]=UAS-RedStinger}6, P{w[+mC]=UAS-FLP.Exel}3, P{w[+mC]=Ubi-p63E(FRT.STOP)Stinger}15F2/+*
Fig. 7e-h: *yw M{vas-int.Dm}zh-2A; dpp-T2A-d2GFP-NLS/Cyo, P23*
Fig. 7i-l: *yw*
Fig. 8a-c: *ptc-Gal4, dpp^{FO}/+; tubGal80ts/UAS-FLP, act5C(FRT.polyA)lacZ.nls*
Fig. 8d-h: *ptc-Gal4, dpp^{FO}/dpp^{FO}; tubGal80ts/UAS-FLP, act5C(FRT.polyA)lacZ.nls*
Fig. 8i-j: *ci-Gal4, dpp^{FO}/dpp^{FO}; tubGal80ts/UAS-FLP, act5C(FRT.polyA)lacZ.nls*
Supplementary Fig. 1a, e: *ptc-Gal4/+*
Supplementary Fig. 1b, f: *ptc-Gal4/+; UAS/LexAop-HA trap/+*
Supplementary Fig. 2a, c, e, g, i: *HA-dpp/HA-dpp, ci>+* (left) and *HA-dpp/HA-dpp, ci>HA trap* (right)
Supplementary Fig. 2k, m, o, q, s: *HA-dpp/+, ci>+* (left) and *HA-dpp/+, ci>Dpp trap* (right)
Supplementary Fig. 3a: *nub-Gal4, ptc-Gal4, HA-dpp/HA-dpp* (control),
Supplementary Fig. 3b: *nub-Gal4, ptc-Gal4, HA-dpp/HA-dpp; UAS/LexAop-HA trap/+*
Supplementary Fig. 4a: *ptc-Gal4, HA-dpp/HA-dpp*
Supplementary Fig. 4b: *ptc-Gal4, HA-dpp/HA-dpp; UAS/LexAop-HA trap/+*

Supplementary Fig. 4c: *nub-Gal4, HA-dpp/+; UAS/LexAop-Dpp trap/+*,
Supplementary Fig. 4e: *nub-Gal4, HA-dpp/HA-dpp; UAS/LexAop-HA trap/+*,
Supplementary Fig. 4f: *nub-Gal4, HA-dpp/HA-dpp; UAS/LexAop-HA trap/UAS-p35*
Supplementary Fig. 4h: *nub-Gal4, HA-dpp/+; UAS/LexAop-Dpp trap/+*
Supplementary Fig. 4i: *nub-Gal4, HA-dpp/+; UAS/LexAop-Dpp trap/UAS-p35*
Supplementary Fig. 5a, b: (control within the cross) *5xQE.DsRed/+; ($tkvHA^{FO}$, ci-Gal4)/($tkvHA^{FO}$); (UAS-FLP)/tubGal80ts*
Supplementary Fig. 5c, d: *5xQE.DsRed/+; $tkvHA^{FO}$, ci-Gal4/$tkvHA^{FO}$; UAS-FLP/tubGal80ts*
Supplementary Fig. 5e, f: (control within the cross) *5xQE.DsRed/+; ($tkvHA^{FO}$)/($tkvHA^{FO}$); +/Hh-Gal4, tubGal80ts*
Supplementary Fig. 5g, h: *5xQE.DsRed/+; $tkvHA^{FO}$/$tkvHA^{FO}$; UAS-FLP/Hh-Gal4, tubGal80ts*
Supplementary Fig. 6a: (control within the cross) *5xQE.DsRed/+; ($tkvHA^{FO}$)/$tkvHA^{FO}$; (Hh-Gal4)/+*
Supplementary Fig. 6b: (experiment) *5xQE.DsRed/+; $tkvHA^{FO}$/$tkvHA^{FO}$; Hh-Gal4/UAS-FLP*
Supplementary Fig. 7a: *5xQE.DsRed/+, dpp^{d8} or dpp^{d12}/+*
Supplementary Fig. 7b: *5xQE.DsRed/+; dpp^{d8}/dpp^{d12}*
Supplementary Fig. 7c: *5xQE.DsRed, brk^{XA}/Y, dpp^{d8} or dpp^{d12}/+*
Supplementary Fig. 7d: *5xQE.DsRed, brk^{XA}/Y, dpp^{d8}/dpp^{d12}*
Supplementary Fig. 8a: *Ollas-HA-dpp, ptc-Gal4/+*
Supplementary Fig. 8b: *Ollas-HA-dpp, ptc-Gal4/+; UAS/LexAop-C9/+*
Supplementary Fig. 8d, h: *ptc-Gal4/+*
Supplementary Fig. 8e, i: *ptc-Gal4/+; UAS/LexAop-C9/+*
Supplementary Fig. 9a: *yw; ptc-Gal4, HA-dpp/+* (identical disc as Fig. 5c)
Supplementary Fig. 9b: *yw; ptc-Gal4, HA-dpp/+; UAS/LexAop-Dpp trap/+* (identical disc as Fig. 5d)
Supplementary Fig. 9c, d: *dpp^{FO}/+; UAS-FLP/tubGal80ts*
Supplementary Fig. 9e: *dpp^{FO}, ci-Gal4/dpp^{FO}; UAS-FLP/tubGal80ts*
Supplementary Fig. 10a: (control) *ptc-Gal4, HA-dpp/+*,
Supplementary Fig. 10b: (Dpp trap) *ptc-Gal4, HA-dpp/+; UAS/LexAop-Dpp trap/+*
Supplementary Fig. 10c: (HA trap) *ptc-Gal4, HA-dpp/HA-dpp; UAS/LexAop-HA trap/+*
Supplementary Fig. 11: *yw M{vas-int.Dm}zh-2A; dpp-T2A-d2GFP-NLS/Cyo, P23*
Supplementary Fig. 12: (control) *ptc-Gal4, HA-dpp/HA-dpp; tubGal80ts/+*, (experiment) *ptc-Gal4, HA-dpp/HA-dpp; UAS/LexAop-HA trap/tubGal80ts*
Supplementary Fig. 13: (control) *$tkvHA^{FO}$/+; UAS-FLP/tubGal80ts*, (experiment) *$tkvHA^{FO}$, ci-Gal4/$tkvHA^{FO}$; UAS-FLP/tubGal80ts*

SUPPLEMENTARY TABLE 2

Primer lists to determine the orientation of the *dpp* genomic fragment insertion.

S25	mCherry-AgeI-F	CCACCGGTCGCCACCATGGTGAGCAAGGGCGA
S85	Dpp mimic-F1	GCGGCCGCCCAAGATCGACCGCTCC
S86	Dpp mimic-R1	CGCGGTGCACAAAAGCCTAGGCGGATGGC

S25/S86 for the right orientation.
S25/S85 for the wrong orientation.